(K,Na)$_2$[AsB$_6$O$_{12}$]$_2$[B$_3$O$_3$(OH)$_3$], a New Microporous Material, and Its Comparison to Teruggite

Yulia A. Pankova [1,2] and Sergey V. Krivovichev [1,3,*]

[1] Department of Crystallography, Institute of Earth Sciences, St. Petersburg State University, University Emb. 7/9, 199034 Saint Petersburg, Russia; yulika1314@gmail.com

[2] Laboratory of Nature-Inspired Technologies and Environmental Safety of the Arctic, Kola Science Centre, Russian Academy of Sciences, Fersmana 14, 184209 Apatity, Russia

[3] Nanomaterials Research Center, Federal Research Center, Kola Science Center, RAS, Fersmana Str. 14, 184209 Apatity, Russia

* Correspondence: s.krivovichev@ksc.ru; Tel.: +7-81555-7-53-50

Abstract: Single crystals of the novel boroarsenate (K,Na)$_2$[As$_2$B$_{12}$O$_{24}$][B$_3$O$_3$(OH)$_3$] (**I**) were obtained using the borax flux method. The crystal structure of **I** was found to be triclinic, *P*-1, *a* = 8.414(5), *b* = 10.173(6), *c* = 15.90(1) Å, α = 79.56(1), β = 78.68(1), γ = 70.91(1), *V* = 1251(1) Å^3, *Z* = 2. The crystal structure of **I** is based upon the novel [AsB$_6$O$_{12}$]$^-$ microporous boroarsenate framework formed by B and As coordination polyhedra. This framework can be subdivided into borate units that are interlinked by AsO$_4$ tetrahedra. In the case of **I**, the borate substructure is a chain consisting of triborate rings, □2Δ, formed by two (BO$_3$) triangles and one (BO$_4$) tetrahedron connected through shared common oxygen atoms. The chains are extended along [0$\overline{1}$1] and are interlinked by (AsO$_4$) tetrahedra in the [011] direction. As a result, the framework has large channels parallel to [100], having an effective diameter of 4.2 × 5.6 Å^2. The channels contain occluded electroneutral ring triborate complexes, [B$_3$O$_3$(OH)$_3$]^0, formed by three (BO$_2$(OH$^-$))$^-$ triangles sharing common O atoms, as well as K$^+$ and Na$^+$ cations. The triborate [B$_3$O$_3$(OH)$_3$]^0 units correspond to similar clusters found in the crystal structure of the α-form of metaboric acid, HBO$_2$. According to information-based complexity calculations, the crystal structure of **I** should be described as complex, with I_G = 5.781 bits/atom and $I_{G,total}$ = 625.950 bits/cell. Teruggite, Ca$_4$Mg[B$_6$As(OH)$_6$O$_{11}$]$_2$(H$_2$O)$_{14}$, the only known boroarsenate of natural origin, has almost twice as much information per unit cell, with $I_{G,total}$ = 1201.992 bits/cell. The observed difference in structural complexity between **I** and teruggite is the consequence of their chemistry (hydration state) and different formation conditions.

Keywords: crystal structure; boroarsenate; microporous framework; structural complexity; Shannon information; terrugite

1. Introduction

Borophosphates and metalloborophosphates constitute an important, chemically and structurally rich family of boron compounds, with more than 220 different structural architectures having been reported to date. The first systematic approach to the structural chemistry of borophosphates was proposed by Kniep et al. [1], who used the dimensionality of complex anions, the B/P ratio, and the type of fundamental building blocks as classification criteria. Later, as the number of compounds steadily grew, the systematics was refined further, additionally taking into account the type of boron polyhedra ((BO$_4$) tetrahedra and/or (BO$_3$) triangles), the degree of protonation (ratio O/OH), and the method of synthesis [2,3]. In contrast to borophosphates, the number of boroarsenates is much smaller, with around a dozen of compounds reported to date [4–11]. Such limited number compared

to that of borophosphates is undoubtedly due to the toxicity of arsenic, which drastically restricts the possible technological applications of boroarsenates. It is, however, interesting that no borophosphates sensu stricto (i.e., compounds containing polyions of linked B and P polyhedra) have been reported as minerals, whereas there is one natural boroarsenate—teruggite, $Ca_4Mg[B_6As(OH)_6O_{11}]_2(H_2O)_{14}$—that was first found in the Loma Blanca borate deposit in the province of Jujuy, Argentina [12]. Later, the mineral was also reported from the Emet borate deposits in Turkey [13] and the El Tatio geothermal field in Chile [14]. In all cases, the formation of teruggite was associated with the activity of borate-rich thermal springs. The crystal structure of teruggite was determined using the crystal from the Emet deposit and was reported as being based upon 0-dimensional $[B_6As(OH)_6O_{11}]^{5-}$ units, consisting of four (BO_4) tetrahedra, two (BO_3) triangles, and one (AsO_4) tetrahedron [15]. It should be noted that there are other minerals that contain both B and As (such as cahnite, $Ca_2[B(OH)_4](AsO_4)$ [16]) or B and P (such as seamanite, $Mn_3[B(OH)_4](PO_4)(OH)_2$ [17–19]), but in their structures, no linkage exists between BO_n and TO_4 polyhedra (n = 3, 4; T = P, As).

The aim of this study is to report on the synthesis and crystal structure of $(K,Na)_2[AsB_6O_{12}]_2[B_3O_3(OH)_3]$ (**I**), a new microporous compound, which is the first boroarsenate containing occluded electroneutral $[B_3O_3(OH)_3]^0$ moieties within its framework channels. We also describe the relations of **I** to teruggite, the only natural boroarsenate.

2. Materials and Methods

2.1. Synthesis

The crystals of **I** were prepared using boric acid as a flux in a closed system. The mixture of $Cu(CH_3COO)_2$, $Na(CH_3COO)\cdot3H_2O$, KH_2AsO_4, and H_3BO_3 taken in the ratio of 1:1:1:20, was ground in an agate mortar. The resulting mixture, together with 100 μL of distilled water, was placed into a stainless-steel autoclave with teflon liner. The autoclave was held at a temperature of 200 °C and autogenous pressure for 7 days and then cooled to room temperature. Needle-shaped, transparent, colorless crystals were found on the surface of the melt, which consisted of H_3BO_3 and some amount of CuB_2O_4 crystals. Semiquantitative chemical analysis using SEM (S-3400N, Hitachi, Tokyo, Japan) indicated the absence in **I** of any other element heavier than O, except K, Na, and As. Several crystals were selected for further crystal structure determination using an optical microscope.

2.2. Crystal Structure Analysis

Several crystals of **I** selected for data collection were mounted on a Bruker APEX II DUO X-ray diffractometer (Karlsruhe, Germany) operated at 50 kV and 40 mA and equipped with the IμS microfocus source. More than a hemisphere of three-dimensional data was collected for each crystal using monochromatic MoK_α X-radiation. From several datasets, one was chosen that demonstrated more or less reliable data, whereas others were neglected due to their poor quality. The unit-cell parameters (Table 1) were refined using the least-squares techniques. The intensity data were integrated and corrected for Lorentz, polarization, and background effects using the Bruker programs APEX and XPREP. An analytical multiscan absorption correction was performed using the Bruker program SADABS. The observed systematic absences were consistent with the space group $P\bar{1}$. The crystal structure was solved and refined using the SHELX program package, which was used for all structural calculations [20]. The refinement converged to R_1 = 0.061 on the basis of 3436 unique observed reflections. No H atoms could be found, due to the observed alkali metal cation disorder in the framework cavities (see below). The final atomic coordinates and isotropic displacement parameters are given in Table 2, and selected interatomic distances are in Table 3. Anisotropic displacement parameters and other details of the data collection and structure refinement are available as a Crystallographic Information File (CIF) included as Supplementary Materials.

Table 1. Crystal data and structure refinement parameters for **I**.

Crystallographic Data	
Crystal system	triclinic
Space group	$P\bar{1}$
a, b, c [Å], α, β, γ [°], V [Å^3]	8.414(5), 10.173(6), 15.90(1), 79.56(1), 78.68(1), 70.91(1), 1251(1)
Z	2
Crystal density (g/cm^3)	2.609
Absorption coefficient (mm^{-1})	9.039
Crystal size/mm^3	$0.37 \times 0.07 \times 0.05$
Data Collection Parameters	
Radiation type, wavelength	MoK_α, 0.71073
2θ angles range, deg.	5.18−59.422
Index ranges	$-9 \leq h \leq 11$
	$-14 \leq k \leq 14$
	$-22 \leq l \leq 22$
Reflections collected	21,483
Independent reflections	7031 [R_{int} = 0.1044, R_{sigma} = 0.1203]
Observed reflections ($>4\sigma F_\sigma$)	3436
Structure Refinement Parameters	
Refinement method	Full-matrix least-square analysis of F^2
Weight coefficients a, b	0.0686, 4.5654
R_1 [$F > 4\sigma(F)$], wR_2 [$F > 4\sigma (F)$]	0.061, 0.144
R_1 [all data], wR_2 [all data]	0.148, 0.184
S	0.954
ρ_{max}, ρ_{min}, $e \cdot$Å^{-3}	1.611/−0.923

Table 2. Atomic coordinates, isotropic displacement parameters (Å^2) and site-occupation factors (s.o.f.) for **I**.

Atom	s.o.f.	x	y	z	U^{eq}
As1	As	0.25014(8)	0.49578(7)	0.00236(4)	0.0163(2)
As2	As	0.75034(8)	0.99316(7)	−0.49276(5)	0.01621(19)
O1	O	0.3335(6)	0.5060(5)	0.0872(3)	0.0217(11)
O2	O	0.1062(5)	0.6462(5)	−0.0285(3)	0.0222(11)
O3	O	0.3657(6)	1.4531(5)	−0.5439(3)	0.0268(12)
O4	O	0.2601(7)	0.9363(5)	−0.0505(3)	0.0306(13)
O5	O	1.0757(6)	0.8610(5)	−0.6022(3)	0.0216(11)
O6	O	0.4249(6)	1.2178(5)	−0.4820(3)	0.0205(11)
O7	O	0.6068(6)	1.0206(5)	−0.4031(3)	0.0207(10)
O8	O	0.8969(5)	0.8423(5)	−0.4651(3)	0.0191(10)
O9	O	0.3925(5)	0.4690(5)	−0.0881(3)	0.0208(11)
O10	O	0.1523(6)	1.6571(5)	−0.4957(3)	0.0224(11)
O11	O	0.2096(7)	1.3482(5)	−0.2455(3)	0.0335(13)
O12	O	0.1311(6)	1.1568(5)	0.0042(3)	0.0191(10)
O13	O	0.8288(6)	1.1271(5)	−0.5304(3)	0.0225(11)
O14	O	0.6672(6)	0.9855(5)	−0.5787(3)	0.0214(11)
O15	O	0.3531(6)	1.1589(5)	−0.3274(3)	0.0188(10)
O16	O	0.1708(6)	0.3611(5)	0.0384(3)	0.0226(11)
O17	O	0.2105(8)	1.1404(5)	−0.1467(4)	0.0401(15)
O18	O	0.2996(7)	1.6575(5)	−0.6402(3)	0.0325(14)
O19	O	0.3999(6)	0.7169(5)	0.0147(3)	0.0188(10)
O20	O	0.3694(6)	0.6635(5)	0.1718(3)	0.0206(11)
O21	O	0.1692(7)	0.8373(6)	0.2533(3)	0.0411(16)
O22	O	0.0972(6)	1.3666(5)	−0.1012(3)	0.0204(11)
O23	O	0.2027(8)	0.8791(6)	0.1037(3)	0.0446(17)

Table 2. *Cont.*

Atom	s.o.f.	x	y	z	U^{eq}
O24	O	0.2877(7)	1.3955(6)	−0.3928(3)	0.0388(15)
O25	O	0.3380(10)	0.3253(8)	0.2813(5)	0.068(2)
O26	O	0.9331(10)	0.6982(8)	−0.2753(5)	0.063(2)
O27	O	0.9550(11)	0.8431(9)	−0.1848(5)	0.081(3)
O28	O	0.6844(10)	0.8290(9)	−0.1912(5)	0.074(3)
O29	O	0.9103(10)	0.5445(8)	−0.3663(5)	0.068(2)
O30	O	0.4197(12)	0.7913(11)	−0.1968(6)	0.094(3)
B1	B	0.2687(10)	1.5892(8)	−0.5574(5)	0.0209(16)
B2	B	0.2880(11)	0.8440(9)	0.0233(5)	0.0264(19)
B3	B	0.4267(9)	0.6100(8)	0.0890(5)	0.0155(16)
B4	B	0.1974(10)	1.0816(8)	−0.0615(5)	0.0240(18)
B5	B	0.4276(9)	1.1083(9)	−0.4103(5)	0.0213(18)
B6	B	0.3588(10)	1.3549(8)	−0.4728(5)	0.0201(17)
B7	B	0.2508(11)	0.7894(9)	0.1775(5)	0.0260(19)
B8	B	0.1747(10)	1.2836(9)	−0.1631(6)	0.0247(19)
B9	B	0.2870(10)	1.2944(9)	−0.3215(5)	0.0244(18)
B10	B	1.0748(10)	0.8074(8)	−0.5110(5)	0.0197(18)
B11	B	1.1827(11)	0.7849(9)	−0.6624(5)	0.0245(19)
B12	B	−0.0751(9)	0.6896(8)	0.0104(5)	0.0163(16)
B13	B	0.1662(15)	0.3618(11)	0.3052(8)	0.045(3)
B14	B	0.8542(14)	0.7964(14)	−0.2181(7)	0.047(3)
B15	B	0.5874(14)	0.7803(15)	−0.2237(7)	0.051(3)
K1/Na1	$K_{0.43}Na_{0.57}$	0.8373(4)	0.0355(4)	0.2656(2)	0.0725(16)
K2	$K_{0.58}$	0.5869(8)	0.4469(5)	0.2792(3)	0.0823(17)
K3	$K_{0.23}$	0.717(2)	0.3281(17)	0.3281(13)	0.108(5)
Na2	$Na_{0.19}$	0.771(3)	0.415(2)	0.2168(16)	0.055(6)

Table 3. Selected interatomic distances (Å) in the crystal structure of **I**.

As1–O1	1.671(5)	As2–O13	1.670(5)	B1–O10	1.352(9)
As1–O2	1.673(5)	As2–O8	1.673(4)	B1—O3	1.360(9)
As1–O16	1.678(5)	As2–O14	1.677(5)	B1–O18	1.392(9)
As1–O9	1.682(5)	As2–O7	1.678(4)	<B1–O>	1.368
<As1–O>	1.676	<As2–O>	1.674		
				B4–O12	1.330(9)
B2–O19	1.340(10)	B3–O20	1.450(9)	B4–O17	1.378(9)
B2–O4	1.371(9)	B3–O19	1.453(8)	B4–O4	1.388(9)
B2–O23	1.385(10)	B3–O9	1.468(8)	<B4–O>	1.365
<B2–O>	1.365	B3–O1	1.516(9)		
		<B3–O>	1.472	B7–O20	1.347(9)
B5–O6	1.441(9)			B7–O21	1.355(10)
B5–O15	1.452(9)	B6–O6	1.345(9)	B7–O23	1.388(9)
B5–O14	1.480(10)	B6–O24	1.371(9)	<B7–O>	1.363
B5–O7	1.494(9)	B6–O3	1.372(8)		
<B5–O>	1.467	<B6–O>	1.363	B10–O10	1.448(9)
				B10–O5	1.454(9)
B8–O22	1.340(10)	B9–O15	1.321(9)	B10–O8	1.489(8)
B8–O17	1.373(9)	B9–O11	1.372(10)	B10–O13	1.502(10)
B8–O11	1.379(9)	B9–O24	1.387(9)	<B10–O>	1.473
<B8-O>	1.364	<B9-O>	1.360		
				B13–O25	1.362(13)

Table 3. *Cont.*

B11–O5	1.342(9)	B12–O22	1.454(8)	B13–O26	1.375(14)
B11–O21	1.362(9)	B12–O12	1.465(9)	B13–O29	1.399(13)
B11–O18	1.381(9)	B12–O16	1.475(9)	<B13–O>	1.379
<B11–O>	1.362	B12–O2	1.481(8)		
		<B12–O>	1.469	K1/Na1–O27	2.487(10)
B14–O27	1.325(14)			K1/Na1–O30	2.591(10)
B14–O28	1.355(13)	B15–O28	1.305(14)	K1/Na1–O14	2.659(6)
B14–O26	1.387(13)	B15–O30	1.366(13)	K1/Na1–O21	2.854(6)
<B14–O>	1.356	B15–O25	1.441(15)	K1/Na1–O15	2.861(6)
		<B15–O>	1.371	K1/Na1–O17	2.989(7)
K2–O25	2.751(10)			K1/Na1–O5	3.093(6)
K2–O20	2.890(7)	K3–O26	2.832(18)	<K1/Na1–O>	2.791
K2–O18	2.910(7)	K3–O13	2.834(17)		
K2–O30	2.977(11)	K3–O10	3.119(18)	Na2–O9	2.58(2)
K2–O9	2.991(7)	K3–O24	3.150(19)	Na2–O11	2.60(2)
K2–O11	3.022(7)	K3–O30	3.15(2)	Na2–O26	2.65(2)
K2–O3	3.051(7)	K3–O3	3.260(19)	Na2–O27	2.92(2)
K2–O24	3.139(8)	<K3–O>	3.106	Na2–O22	2.98(2)
<K2–O>	2.966			<Na2–O>	2.746

2.3. Structural Complexity Calculations

The structural complexity parameters for **I** and other boroarsenates and borophosphates were estimated as follows. The amounts of structural Shannon information per atom ($^{str}I_G$) and per unit cell ($^{str}I_{G,total}$) were calculated using the approach developed by Krivovichev [21–24] according to the following equations:

$$^{str}I_G = -\sum_{i=1}^{k} p_i \log_2 p_i \qquad \text{(bits/atom)} \qquad (1)$$

$$^{str}I_G = -v\sum_{i=1}^{k} p_i \log_2 p_i \qquad \text{(bits/cell)} \qquad (2)$$

where k is the number of different crystallographic orbits (independent crystallographic Wyckoff sites) in the structure, and p_i is calculated according to the formula:

$$p_i = m_i/v \qquad (3)$$

where m_i is a multiplicity of a crystallographic orbit (i.e., the number of atoms of a specific Wyckoff site in the reduced unit cell), and v is the total number of atoms in the reduced unit cell.

In total, 237 crystal structures of borophosphates and boroarsenates were analyzed from the viewpoint of their information-based structural complexity (see Supplementary Materials). All structure complexity calculations were performed by means of the TOPOS program package developed by Blatov et al. [25].

3. Results

Structure Description

The crystal structure of **I** was found to be based upon the novel $[AsB_6O_{12}]^-$ microporous boroarsenate framework (Figure 1) formed by B and As coordination polyhedra. As is usual for borophosphates and boroarsenates [1–3], the framework can be subdivided into borate units that are interlinked by AsO_4 tetrahedra. In the case of **I**, the borate substructure is a chain consisting of triborate rings, □2Δ, formed by two (BO_3) triangles and one (BO_4) tetrahedron connected through shared common oxygen atoms (Figure 2). The chains are extended along $[0\bar{1}1]$ and are interlinked by (AsO_4) tetrahedra in the [011] direction (Figure 3). As a result, the framework has large channels parallel to

[100], having the absolute diameter of 6.9 × 8.3 Å^2 or an effective diameter of 4.2 × 5.6 Å^2, taking into account the average radius of the O^{2-} anion equal to 1.35 Å. The channels are large enough to contain occluded electroneutral ring triborate complexes, [B$_3$O$_3$(OH)$_3$]^0, formed by three (BO$_2$(OH))$^-$ triangles sharing common O atoms, as well as K$^+$ and Na$^+$ cations.
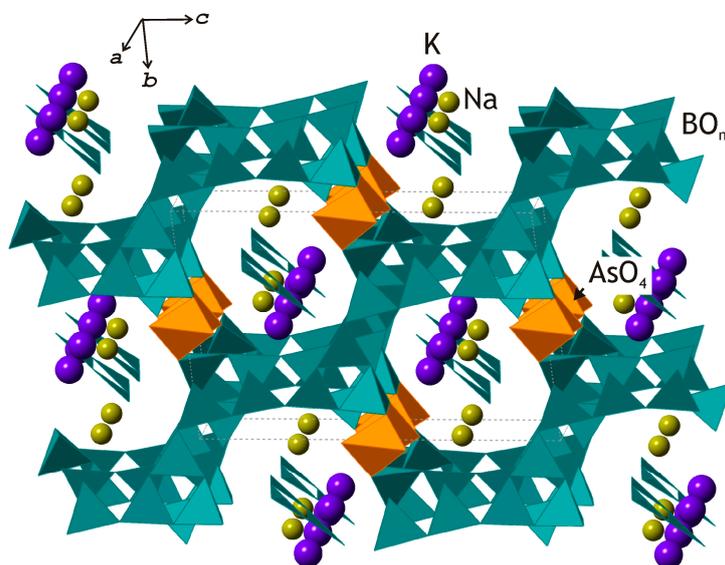
Figure 1. The crystal structure of **I** is based upon a complex heteropolyhedral framework formed by B and As polyhedra.
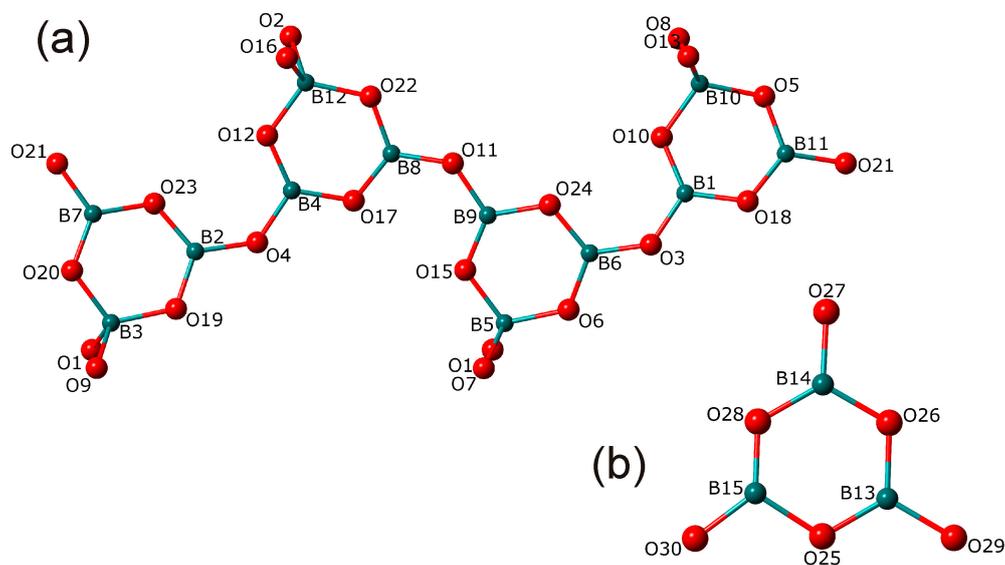
Figure 2. The borate structural units in **I**: the [B$_{12}$O$_{24}$]$^{12-}$ chain (**a**) and the B-O skeleton of the protonated triborate unit, [B$_3$O$_3$(OH)$_3$]^0 (**b**).

There are two independent As sites in the crystal structure of I, which are coordinated tetrahedrally, with the average <As1–O> and <As2–O> distances equal to 1.676 and 1.674 Å, respectively. These values are slightly shorter than the average value of 1.685 Å reported for arsenate minerals by Majzlan et al. [26]. There are 14 crystallographically independent B sites in the crystal structure of **I**. The B1–B12 atoms belong to the chains of triborate groups, whereas the B13 and B14 atoms constitute diborate complexes. The B3, B5, B10, and B12 atoms are tetrahedrally coordinated (and denoted as B$^\square$), with the average <B$^\square$–O> bond lengths in the range of 1.462–1.473 Å. The rest of the B atoms are triangularly coordinated (B$^\Delta$), with the average <B$^\Delta$–O> lengths for the B atoms

of triborate groups varying from 1.359 to 1.371 Å. The average <B–O> bond lengths are in general agreement with the average values of 1.370 and 1.476 Å given for (BO$_3$) and (BO$_4$) groups, respectively, by Hawthorne et al. [27]. The average <B$^\Delta$–O> lengths for the intersitial triborate complexes are 1.379, 1.356, and 1.371 Å for B13, B14, and B15, respectively. The rather unusual observed values are undoubtedly the result of the high mobility of the triborate units. The isotropic displacement parameters for their O atoms are approximately two times higher than those of the framework O atoms, and the same was also observed for the B atoms (Table 3). Filatov and Bubnova [28] analyzed variations of B–O bond lengths for the □2Δ triborate groups in inorganic borates. They distinguished two types of bridging O atoms in these groups: O atoms shared between two (BO$_3$) triangles, $^\Delta$O$^\Delta$, and O atoms shared between (BO$_3$) triangle and (BO$_4$) tetrahedron, $^\Delta$O$^\square$. Accordingly, there are three types of B–O bonds to bridging O atoms: B$^\Delta$–$^\Delta$O$^\Delta$, B$^\Delta$–$^\Delta$O$^\square$, and B$^\square$–$^\Delta$O$^\square$. The average bond distances for these bonds are 1.374, 1.347, and 1.471 Å [28]. For the crystal structure of **I**, the analogous parameters were determined as (variations of individual bond lengths are given in brackets): 1.382 (1.370–1.393), 1.339 (1.330–1.352), and 1.451 (1.440–1.461) Å, respectively. These values are in agreement with the general tendency of bond-length variations described in [28].
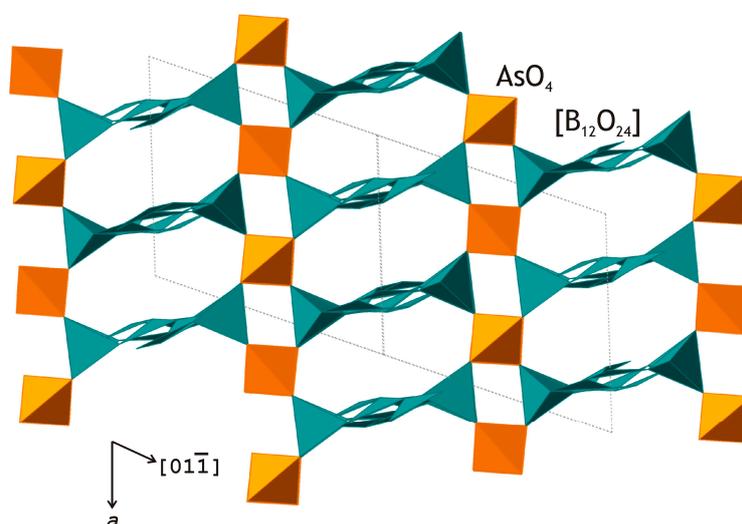

Figure 3. The microporous boroarsenate framework in the crystal structure of **I**, composed of chains of boron polyhedra interlinked by AsO$_4$ tetrahedra.

The crystal structure contains a total of four alkali metal sites: one K, two Na, and one with mixed K–Na occupancy. The K1/Na1 site has a sevenfold coordination with the *Me*–O bond lengths (*Me* = Na, K) in the range of 2.487–3.093 Å. The coordination numbers for the K2 and K3 sites (occupation factors of 0.58 and 0.23, respectively) are eight and six, respectively, with average *Me*–O distances of 2.966 and 3.106 Å, respectively. The Na2 site (with 19% occupancy) is coordinated by five O atoms with the *Me*–O distances in the range of 2.58–2.98 Å.

4. Discussion

The construction of the boroarsenate framework agrees well with the bond-valence matching principle formulated by Hawthorne [29]. The linkage between As and B polyhedra involves tetrahedrally coordinated As^{5+} and B^{3+}, since the [4]As^{5+}–O and [4]B^{3+}–O average bond valences are equal to 1.25 and 0.75 valence units (v.u.), which provides a perfect matching for the valence saturation of O^{2-} anions (1.25 + 0.75 = 2.00 v.u.).

The triborate [B$_3$O$_3$(OH)$_3$]^0 units located in the framework cavities of the boroarsenate framework in **I** correspond to the similar clusters found in the crystal structure of the α-form of metaboric acid, HBO$_2$ [30].

According to the information-based complexity calculations, the crystal structure of **I** should be described as complex, with I_G = 5.781 bits/atom and $I_{G,total}$ = 625.950 bits/cell (after the procedure of H-correction that takes into account the presence of H atoms [31]). It is of interest that teruggite, $Ca_4Mg[B_6As(OH)_6O_{11}]_2(H_2O)_{14}$, the only known boroarsenate of natural origin, has almost twice as much information per unit cell, with $I_{G,total}$ = 1201.992 bits/cell.

As mentioned above, the crystal structure of teruggite [15] is based upon planar 0-dimensional $[B_6As(OH)_6O_{11}]^{5-}$ units, consisting of four (BO_4) tetrahedra, two (BO_3) triangles, and one (AsO_4) tetrahedron (Figure 4a), which share one common O atom with the peripheral (BO_4) tetrahedron (Figure 4b,c). The structure of teruggite contains two symmetrically independent Ca atoms coordinated by eight O atoms each. The CaO_8 polyhedra link the boroarsenate units into a three-dimensional open framework with channels that are extended along the *c* axis and accommodate isolated $Mg(H_2O)_6$ octahedra. The high structural complexity of teruggite is due to the presence of rather large finite-cluster units and high hydration states (14 H_2O molecules per formula unit). The observed difference in structural complexity between **I** and teruggite is the consequence of their chemistry (hydration state) and different formation conditions. Teruggite was crystallized from low-temperature borate-rich aqueous solutions, whereas **I** was obtained from boric acid flux at 200 °C.
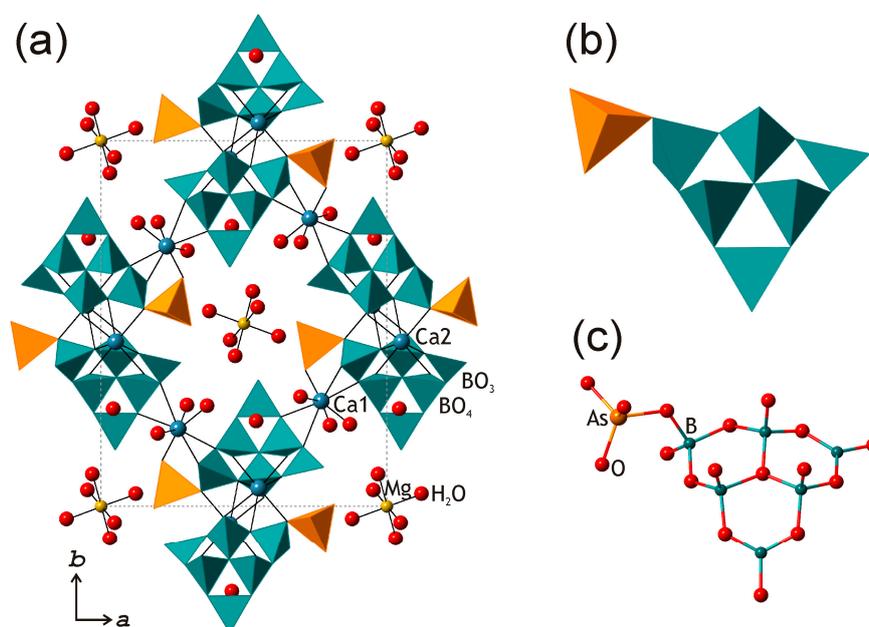

Figure 4. The crystal structure of teruggite (**a**) and the $[B_6As(OH)_6O_{11}]^{5-}$ unit shown in polyhedral (**b**) and ball-and-stick (**c**) representations.

References

1. Kniep, R.; Engelhart, H.; Hauf, C. A first approach to borophosphate structural chemistry. *Chem. Mater.* **1998**, *10*, 2930–2934. [CrossRef]

2. Ewald, B.; Huang, Y.-X.; Kniep, R. Strucrural chemistry of borophosphates, metalloborophosphates and related compounds. *Z. Anorg. Allg. Chem.* **2007**, *633*, 1517–1540. [CrossRef]

3. Li, M.; Verena-Mudring, A. New developments in synthesis, structure, and applications of borophosphates and metalloborophosphates. *Cryst. Growth. Des.* **2016**, *16*, 2441–2458. [CrossRef]

4. Schulze, G.E.R. Die Kristallstruktur von BPO_4 und $BAsO_4$. *Z. Phys. Chem. B.* **1934**, *24*, 215–240. [CrossRef]

5. Driss, A.; Jouini, T. Structure de $Na_2AlBAs_4O_{14}$, un aluminoboroarseniate condense. *Acta Crystallogr.* **1988**, *C44*, 791–794. [CrossRef]

6. Bluhm, K.; Park, C.-H. $Pb_6(AsO_4)(B(AsO_4)_4)$-ein neuartiger Kristallstrukturtyp im System $PbO/B_2O_3/As_2O_5$ mit einem Beitrag ueber $Pb(BAsO_5)$. *Z. Naturforsch. B* **1996**, *51*, 313–318.

7. Haines, J.; Cambon, O.; Astier, R.; Fertey, P.; Chateau, C. Crystal structures of alpha-quartz homeotypes boron phosphate and boron arsenate: Structure-property relationships. *Z. Kristallogr.-Cryst. Mater.* **2004**, *219*, 32–37. [CrossRef]

8. Wiggin, S.B.; Weller, M.T. Boroarsenates: A framework motif and family templated on cations and anions. *J. Am. Chem. Soc.* **2005**, *127*, 17172–17173. [CrossRef]

9. Lieb, A.; Weller, M.T. $NH_4[BAsO_4F]$—A new layer fluoro-boroarsenate with a silicate related topology. *Z. Anorg. Allg. Chem.* **2009**, *635*, 1877–1881. [CrossRef]

10. Lieb, A.; Weller, M.T. $(NH_4)_2[BAs_2O_7(OH)]$—A framework compound with two polymorphs. *Z. Anorg. Allg. Chem.* **2009**, *636*, 2085. [CrossRef]

11. Lieb, A.; Weller, M.T. Determination of the hydrogen positions in the novel barium boroarsenate $Ba[B_2As_2O_8(OH)_2]$ by combined single crystal X-ray and powder neutron investigations. *Z. Anorg. Allg. Chem.* **2017**, *643*, 1649–1653. [CrossRef]

12. Aristarain, L.F.; Hurlut, C.S. Teruggite, $4CaO \cdot MgO \cdot 6B_2O_3 \cdot As_2O_5 \cdot 18H_2O$, a new mineral from Jujuy, Argentina. *Am. Mineral.* **1968**, *53*, 1815–1827.

13. Helvaci, C. Occurrence of rare borate minerals: Veatchite-A, tunellite, teruggite and cahnite in the Emet borate deposits, Turkey. *Mineral. Dep.* **1984**, *19*, 217–226. [CrossRef]

14. Garcia-Valles, M.; Fernandez-Turiel, J.L.; Gimeno-Torrente, D.; Saavedra-Alonso, J.; Martinez-Manent, S. Mineralogical characterization of silica sinters from the El Tatio geothermal field, Chile. *Am. Mineral.* **2008**, *93*, 1373–1383. [CrossRef]

15. Negro, A.D.; Kumbasar, I.; Ungaretti, L. The crystal structure of teruggite. *Am. Mineral.* **1973**, *58*, 1034–1043.

16. Prewitt, C.T.; Buerger, M.J. The crystal structure of cahnite, $Ca_2BAsO_4(OH)_4$. *Am. Mineral.* **1961**, *46*, 1077–1085.

17. Kurkutova, E.N.; Rau, V.G.; Rumanova, I.M. Crystalline structure of seamanite $Mn_3(PO_4/BO_3)(H_2O)_3 = Mn_3(PO_3OH)(BO(OH)_3)(OH)_2$. *Dokl. Akad. Nauk. SSSR* **1971**, *197*, 1070–1073. (In Russian)

18. Moore, P.B.; Ghose, S. A novel face-sharing octahedral trimer in the crystal structure of seamanite. *Am. Mineral.* **1971**, *56*, 1527–1538.

19. Huminicki, D.M.C.; Hawthorne, F.C. Hydrogen bonding in the crystal structure of seamanite. *Can. Mineral.* **2002**, *40*, 923–928. [CrossRef]

20. Sheldrick, G.M. A short history of SHELX. *Acta Crystallogr.* **2008**, *A64*, 112–122. [CrossRef]

21. Krivovichev, S.V. Topological complexity of crystal structures: Quantitative approach. *Acta Crystallogr. Sect. A* **2012**, *68*, 393–398. [CrossRef] [PubMed]

22. Krivovichev, S.V. Structural complexity of minerals: Information storage and processing in the mineral world. *Mineral. Mag.* **2013**, *77*, 275–326. [CrossRef]

23. Krivovichev, S.V. Structural complexity and configurational entropy of crystalline solids. *Acta Crystallogr. Sect. B* **2016**, *72*, 274–276. [CrossRef] [PubMed]

24. Krivovichev, S.V. Ladders of information: What contributes to the structural complexity of inorganic crystals. *Z. Kristallogr.* **2018**, *233*, 155–161. [CrossRef]

25. Blatov, V.A.; Shevchenko, A.P.; Proserpio, D.M. Applied topological analysis of crystal structures with the program package ToposPro. *Cryst. Growth Des.* **2014**, *14*, 3576–3586. [CrossRef]

26. Majzlan, J.; Drahota, P.; Filippi, M. Paragenesis and crystal chemistry of arsenate minerals. *Rev. Mineral. Geochem.* **2014**, *79*, 17–184. [CrossRef]

27. Hawthorne, F.C.; Burns, P.C.; Grice, J.D. The crystal chemistry of boron. *Rev. Mineral. Geochem.* **1996**, *33*, 41–115.

28. Filatov, S.K.; Bubnova, R.S. Borate crystal chemistry. *Phys. Chem. Glasses.* **2000**, *41*, 216–224.

29. Hawthorne, F.C. A bond-topological approach to theoretical mineralogy: Crystal structure, chemical composition and chemical reactions. *Phys. Chem. Miner.* **2012**, *39*, 841–874. [CrossRef]

30. Peters, C.R.; Milberg, M.E. The refined structure of orthorhombic metaboric acid. *Acta Crystallogr.* **1964**, *17*, 229–234. [CrossRef]

31. Pankova, Y.A.; Gorelova, L.A.; Krivovichev, S.V.; Pekov, I.V. The crystal structure of ginorite, $Ca_2[B_{14}O_{20}(OH)_6]*5H_2O$, and the analysis of dimensional reduction and structural complexity in the $CaO–B_2O_3–H_2O$ system. *Eur. J. Mineral.* **2018**, *30*, 277–287. [CrossRef]